

Two Approaches to Electronically Scanned 3D Imaging Using cMUTs

Chris Daft, Satchi Panda, Paul Wagner and Igal Ladabaum
Siemens Medical Solutions
Mountain View, California, USA.
daft@ieee.org

Abstract—Capacitive micromachined ultrasonic transducers (cMUTs) introduce new degrees of freedom in transducer design. For example, it is easy to make elements of any size, and electronics may be integrated directly under the transducer element. These characteristics derive from lithographic manufacturing on a silicon substrate, and the use of a low-temperature surface micromachining process. They are particularly helpful in creating 2D arrays for electronically scanned volume imaging. This paper describes two contrasting ways to achieve volume data acquisition. In bias voltage scanning, we create a Fresnel elevation focus using a crossed electrode design with traditional azimuth beam formation. Then using the bias voltage dependence of k_T in a cMUT, N^2 element connections can be reduced to $2N$. Such a scheme is especially useful in high frequency linear scanning, where N can exceed 200 elements. Measurements and images from a prototype probe are presented. We also describe a method to achieve fully sampled 2D receive apertures with autonomous elements using monolithically integrated electronics. This achieves spatial Nyquist sampling in both array dimensions, with arbitrary element delay and amplitude control. It allows much more of the information in the field returning to the probe to be retrieved by the imager, causing improvements in image quality and diagnostic confidence.

Keywords: medical ultrasound; 3D; silicon ultrasound, cMUT; MEMS; capacitive micromachined transducer; volume imaging.

I. INTRODUCTION

3D imaging *via* bias voltage scanning and Fresnel focusing takes advantage of the ease with which elements of any size can be created lithographically [1]. This article presents new measurements from bias scanned arrays, and images showing the clinical utility of coronal planes with high resolution in all scanning dimensions. The small element area and large number of elements improve image quality, while the relatively low interconnect count makes for a straightforward probe design. These new transducers extend the frequency range attainable with purely electronic scanning beyond commercially available low-frequency cardiac arrays. Their linear scan format is helpful in applications such as breast and small parts imaging.

Integration of cMUTs and electronics was also discussed in [1]. The advantages of monolithic integration are shown in this paper through a fully-sampled 2D array design with autonomous element control and full channel read-out to the system. The advantages of receiving a complete data set

include practical phase aberration, 3D motion tracking, 3D elastography, vector flow and high volume rates. In our probe, each 2D array element has a preamplifier, time-gain control and sample-and-hold circuit positioned directly under the element. The signal at the element is periodically measured. Sampled values from a group of elements are multiplexed together and brought off the chip using a flexible circuit. We have found it practical to implement such a design on an SiGe BiCMOS semiconductor process. Such parallel data collection from thousands of channels offers numerous possibilities for improving clinical workflow and patient management.

II. CHARACTERIZATION OF BIAS SCANNED ARRAYS

Bias scanned transducers using a Fresnel focus have been described in [2]. They rely on the dependence of k_T on bias voltage [3]. Advantages of these arrays over 1D “wobblers” include beam accuracy from electronic scanning, reliability from the lack of moving parts, and improved isotropy of the voxel through multiple focal zones. While traditional beam formation occurs in the azimuth dimension, the phase and amplitude in elevation are controlled by a bias voltage pattern. Figure 1 illustrates one such design.

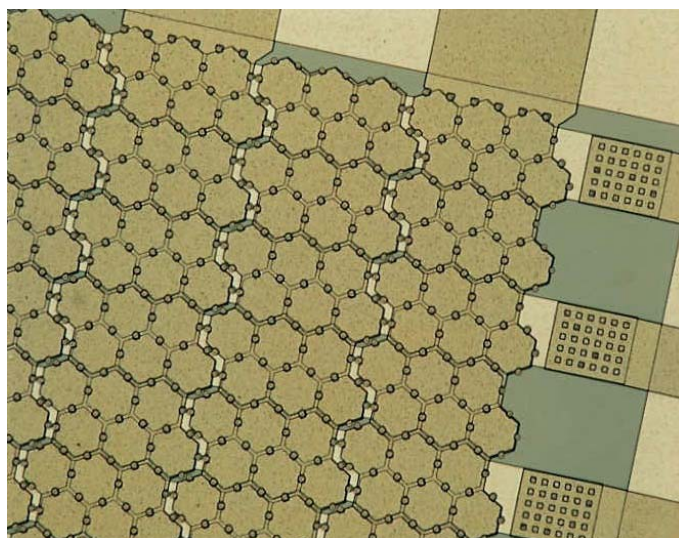


Figure 1. Micrograph of bias scanned array (field of view 0.9 x 0.7 mm). Acoustic elements are defined by the intersection of the vertical and horizontal electrodes. In this design six drums form each 2D element. The array performs a linear scan with a center frequency around 9 MHz.

A. Directivity of elements

Since our array's impulse response and output pressure are as expected and satisfactory, this paper reports on the directivity and bandwidth of the crossed electrode design. Figure 2 shows the angular response of an average element.

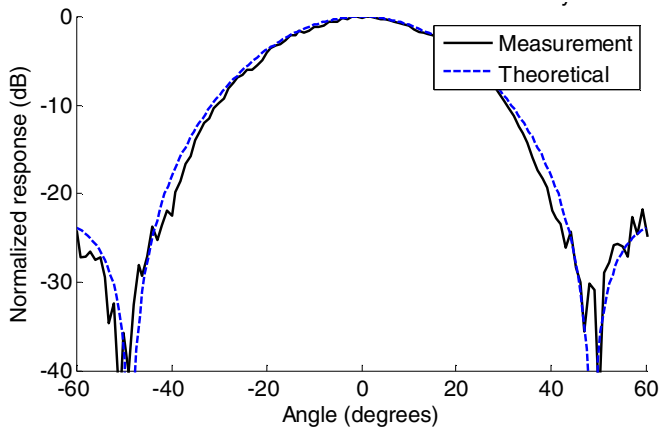


Figure 2. Directivity of an 0.2 mm array element at 10 MHz. The data are close to the theoretical value of $\text{sinc}(w \sin\theta / \lambda) \cos\theta$, where w is the pitch. The smooth curve indicates low levels of unwanted modes and crosstalk.

Element directivity is a key parameter in transducer design: besides affecting steering, it controls resolution by setting a lower limit on the achievable F-number. While cMUTs are mechanically simpler than ceramic transducers due to the lack of conventional backing and matching layers, various types of parasitic modes and surface waves exist natively [4] and require suppression. This smooth response at the theoretical width [5] implies we have successfully removed these modes.

B. Loading impedance and bandwidth

The cMUT's bandwidth and mechanical impedance is determined by characteristics of its electrical environment, in addition to drum parameters such as radius, thickness and stress. Figure 3 shows an interesting effect that has not been widely published for medical arrays: the bandwidth depends on the number of transmit elements connected in parallel.

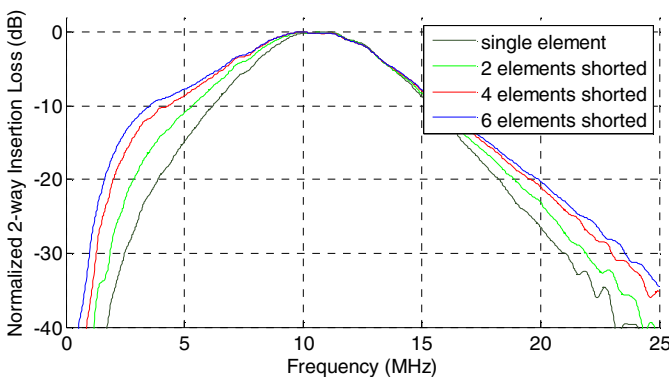


Figure 3. Effect of number of elements connected in parallel on bandwidth. Differences are due to the complex loading impedance. Note that the 50 Ω measurement setup used for these graphs does not optimize element bandwidth as an imager would, but is valid for relative measurements.

When large groups of elements are shorted, the specific tissue loading impedance is 1.5 MRayl and purely real. This is also true for larger apertures with beamforming, as long as the incremental phase shift between adjacent elements is less than $\pi/4$. But for thinner strips (figure 4) the tissue loading becomes reactive and its magnitude falls [6]. Then more pressure is dropped across the imaginary tissue impedance, reducing the actual pressure transmitted.

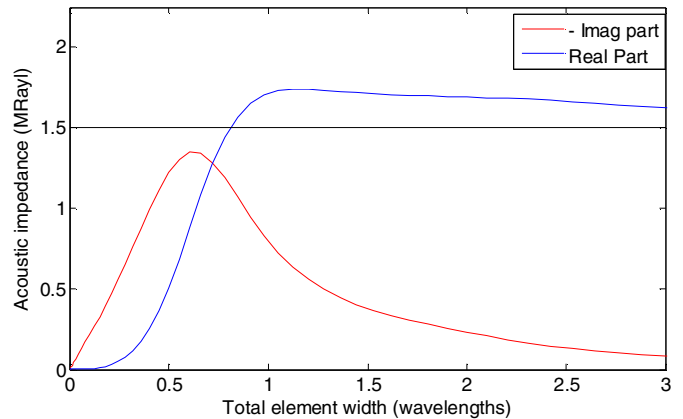


Figure 4. Effect of element width on tissue loading impedance for our design. For large widths the real part asymptotically approaches 1.5 MRayl.

C. Human images

We imaged the leg of a normal volunteer to demonstrate *in-vivo* performance. Figure 5 is a standard B-scan, with axes of azimuth and depth, while figure 6 is a coronal image, or C-plane, of azimuth and elevation at constant depth.

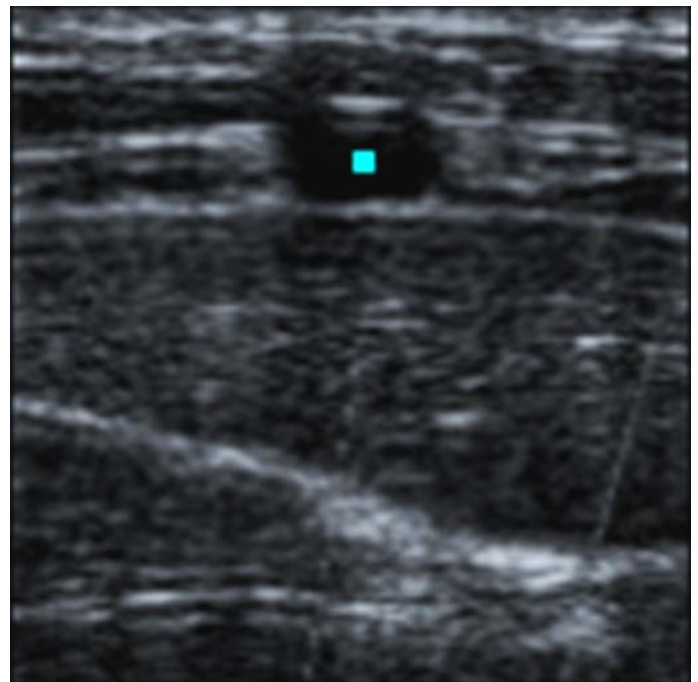


Figure 5. B-scan of leg vessel at 9 MHz. Image dimensions are 4 x 4 cm, and the vessel is transverse to the scan plane. The blue dot, placed in the center of the vessel, indicates the depth of the C-plane of figure 5.

The novel orientation of figure 6 shows a good deal of anatomical detail. This view avoids the difficult mental reconstruction performed by physicians from a set of B-scans, where depth is necessarily one of the image coordinates.

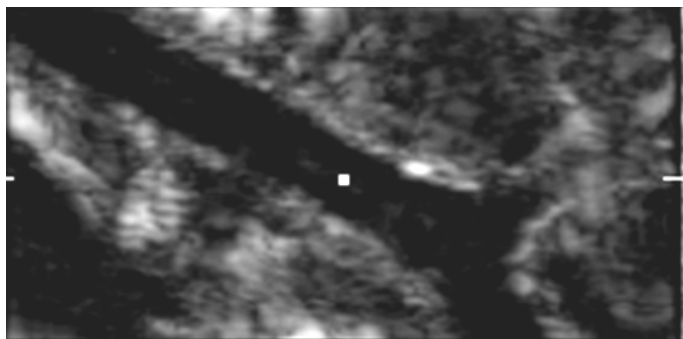


Figure 6. Coronal plane with unusually clear view of leg vein, taken from the same volume acquisition as figure 5. Field of view is 4 x 2 cm and depth is 1 cm. This constant-depth plane cannot be obtained with a 1D array.

III. MONOLITHIC INTEGRATION

While bias scanning has the virtue of simplicity, a perennial goal in ultrasound is to make a fully sampled 2D array with autonomous elements. The rest of this paper investigates how cMUTs enable this advance, focusing on receive processing. Since 2D array fabrication is straightforward in silicon, the problem becomes one of data rate and interconnect. Too much information is created in too small an area for traditional solutions. Array sparseness loses information, increasing sidelobes and reducing SNR. Opportunities for channel-domain processing are also largely lost. Any traditional interconnect is problematic for even a 1000-channel array, while the elements' high impedance precludes driving a cable. If there are N elements in the azimuth and elevation directions of the array, N^2 outputs need to be read out into the ultrasound system. Field-of-view and spatial sampling considerations, particularly in radiology, dictate that $N^2 > 4000$. It is impractical for the number of cables to increase from the common maximum of around 200 while providing a probe which can be manipulated by a sonographer. Aperture size cannot be reduced without severe penetration and resolution loss. What is needed is a method for reading out data from large numbers of transducer elements into ~200 cables.

A. Receiver electronics beneath the 2D element

We have taken advantage of our low-temperature cMUT process to create devices directly above an integrated circuit, with electrical connection through the final IC passivation. The micromachining does not damage the underlying electronics [7]. It solves the interconnect problem by creating a path of only a few micrometers to the circuitry, which is miniaturized so that all processing is confined to the footprint of the element (figure 7). Meeting this constraint makes the design of the metal layers in the IC possible, since nowhere are N^2 signals dealt with outside of the element where the signal is generated. A further advantage of this smallest possible interconnect path from the element to the preamplifier is signal integrity. 2D elements have impedance magnitudes of tens of $k\Omega$, and the

proximity of the preamplifier maximizes SNR and minimizes electrical crosstalk even for such high impedances.

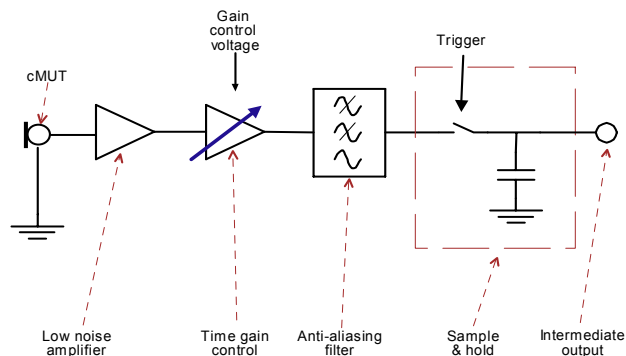


Figure 7. Signal processing integrated beneath a single cMUT element. Intermediate outputs combine at the end of each block of elements (fig. 7.)

The cMUT element is first connected to an amplifier with a high input impedance and low noise. This raises the signal level above the thermal noise floor while also decreasing its impedance, so the subsequent circuitry is more straightforward. The output of this amplifier is connected to a variable-gain stage. As in most ultrasound receivers, this stage decreases the dynamic range requirements of the electronics following by increasing its gain with time, as the acoustic pulse is attenuated through the body. An anti-aliasing filter follows this time-gain control, to eliminate frequency content in the signal above the Nyquist frequency. The slow roll-off of the cMUT above its resonant frequency necessitates special care in the design of this filter. The Nyquist frequency is set by the clock rate of the next stage, a sample and hold circuit. After this processing, an amplified and sampled signal is available at the intermediate output under each 2-D array element for the remainder of each sample period. We then time-domain multiplex the elements to create a higher frequency analog output that flows through a driver to the system A/D converters (figure 8).

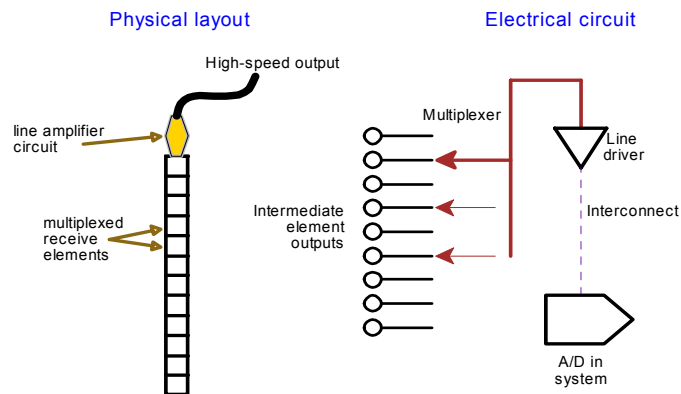


Figure 8. One method to multiplex the outputs from the sub-element electronics. This is implemented in the IC pictured in figure 9. It leverages the ability of standard imaging coaxial cables to transmit higher bandwidths than are typically used in imaging.

The analog multiplexer cycles through a group of elements' sampled voltages and creates a composite waveform. In it,

each sampled voltage exists for a much shorter time—the sample period divided by the multiplexing factor. At the end of each element’s time slice, the output slews swiftly to the appropriate value for the next element. This section is followed by a line driver whose purpose is to precisely couple the output voltage through the interconnect to the A/D. Accurate impedance matching and equalization achieves the specified level of inter-symbol interference across the interconnect to the imager.

B. Practical realization

Figure 9 illustrates one cell of the ASIC layout we designed to implement the circuits of figures 7 and 8. This design multiplexes 12 elements together with a 20 MHz sampling rate, so that the A/D converters are clocked synchronously with the multiplexers at 240 MHz. A 12-fold decrease in channel count makes 2400-element probes feasible; typical ultrasound coaxial cables can transmit data at this bandwidth with appropriate equalization. In the future the multiplexing factor can increase to achieve fully satisfactory element counts, but the principle remains the same.

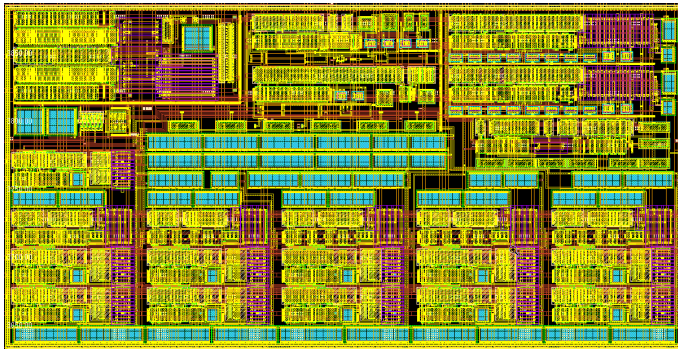


Figure 9. Implementation of sub-cMUT circuitry using a SiGe BiCMOS process. Crucially, the dimensions of the circuit are less than that of an element. This avoids routing the individual element signals around the chip.

After A/D conversion, the data from each transducer are stored in a memory where channel-domain processing such as aberration correction can take place. Then the standard scaling, delay and summation calculation completes the beam formation. Flow estimation and display processing are handled similarly to existing 3D systems.

CONCLUSIONS

We have reported further characterization work on crossed-electrode, bias-scanned arrays. These offer a straightforward method to create high frequency 3D volumes with more isotropic voxel size than “wobbler” arrays. Multiple focal zones in elevation as well as azimuth are mainly responsible for this. Methods to optimize the beam profile and enable accurate harmonic imaging with bias scanning have recently been noted

[8]. Given this potential, it is gratifying that these traditional transducer measurements harbor no unpleasant surprises.

Integration of cMUT transducers with electronics has been discussed as a solution for 2D array interconnect issues for some considerable time, and alternative approaches have been described [9]. We have presented a method modeled on telecommunications techniques (time-domain multiplexing, or TDM) that addresses the problem of the density of information created by a fully-sampled 2D array in receive mode. Other 2D array designs [10] involve beam formation in the transducer handle to reduce the cable count. The present implementation preserves the data from each channel in order to derive maximal information from the received pressure field.

ACKNOWLEDGEMENTS

Many people have contributed to this work, including Kirti Patel, Bill Buchele, Brett Bymaster, Steve Barnes, Sean Hansen, Chuck Bradley, Heman Chu, Kathy Jackson, Joe Lee, Albert Mique, Keith Wong, Alissa Fitzgerald, John Eaton and Daniel da Graca. We are very grateful for their help.

REFERENCES

- [1] Daft, C., Wagner, P., Bymaster, B., Panda, S., Patel, K. and Ladabaum, I., “cMUTs and electronics for 2D and 3D imaging: Monolithic integration, in-handle chip sets and system implications,” *Proc. 2005 IEEE Ultrasonics Symposium*, 463-474.
- [2] Daft, C., Wagner, P., Panda, S. and Ladabaum, I., “Elevation beam profile control with bias polarity patterns applied to microfabricated ultrasound transducers,” *Proc. 2003 IEEE Ultrasonics Symposium*, 1578-1581.
- [3] Yaralioglu, G.G., Ergun, A.S., Bayram, B., Haeggstrom, E. and Khuri-Yakub, B.T., “Calculation and measurement of electromechanical coupling coefficient of capacitive micromachined ultrasonic transducers,” *IEEE Trans. UFFC* **50**(4), 449-456, 2003.
- [4] Wojcik, G., Mould, J., Reynolds, P., Fitzgerald, A., Wagner, P. and Ladabaum, I., “Time-domain models of MUT array cross-talk in silicon substrates,” *Proc. 2000 IEEE Ultrasonics Symposium*, 909-914.
- [5] Selfridge, A.R., Kino, G.S., and Khuri-Yakub, B.T., “A theory for the radiation pattern of a narrow strip acoustic transducer,” *Appl. Phys. Lett.*, **37**, 35-36, 1980.
- [6] Levine, H., “On the Radiation Impedance of a Rectangular Piston,” *J. Sound Vibration* **89**(4), 447-455, 1983.
- [7] Daft, C., Calmes, S., da Graca, D., Patel, K., Wagner, P. and Ladabaum, I., “Microfabricated ultrasonic transducers monolithically integrated with high voltage electronics,” *Proc. 2004 IEEE Ultrasonics Symposium*, 493-496.
- [8] Panda, S., Wagner, P., Daft, C. and Ladabaum, I., “Method and apparatus for improving the performance of capacitive acoustic transducers using bias polarity control and multiple firings,” US Patent Application 20060173342, published 8/6/06.
- [9] Erguri, A.S., Huang, Y., Zhuang, X., Oralkan, O., Yaralioglu, G.G. and Khuri-Yakub, B.T., “Capacitive micromachined ultrasonic transducers: fabrication technology,” *IEEE Trans. UFFC* **52**(12), 2242-2258, 2005.
- [10] Savord, B. and Solomon, R., “Fully sampled matrix transducer for real time 3D ultrasonic imaging,” *Proc. 2003 IEEE Ultrasonics Symposium*, 945-953.